www.advmatinterfaces.de

# **Dual-Responsive Supramolecular Antimicrobial Coating Based on Host-Guest Recognition**

Yiting Wang, Gangyang Wang, Yifeng Ni, Jiahui Zhou, Shuaibing Wang, Yucong Gu, Dong Zhang, Si Yu Zheng,\* Zi Liang Wu, Qiang Zheng, Jie Zheng,\* and Jintao Yang\*

The adhesion and proliferation of the bacteria on biomedical surfaces have posed a great threat to patients. Developing a class of renewable bactericidal surface with excellent bacteria release capability is crucial for elongating the service life of the biomedical devices. However, releasing the bacteria fast and frequently is usually a trade-off with releasing them thoroughly and completely regenerating the surface. Herein, a temperature/light dual-responsive antimicrobial coating is developed. The cyclodextrin (CD)-contained antifouling macromolecule and the thermal-responsive azobenzene-contained macromolecule are assembled on the CDs-modified surface, combined with additional silver nanoparticles. The surface exhibits low bacteria attachments of  $9.30 \times 10^5$  cells cm<sup>-2</sup> (E. coli, 120 h), high bactericidal efficiency of  $\approx 96.3\%$ . Meanwhile, ≈86.9% of the attached bacteria can be released from the surface rapidly in response to temperature, and the residues can be thoroughly removed by irradiating UV irradiation (release ratio ≈91.0%). The functions of the surface can be resumed by switching the host-guest network via light regulation. The 3<sup>rd</sup> regenerated surface still maintains low bacteria density of 12.4 × 10<sup>5</sup> cells cm<sup>-2</sup>, bacteria killing ratio of ≈95.0%, and bacteria release rate of ≈95.7%. The work is supposed to provide a new insight into the design of multifunctional antibacterial surface and broaden their applications.

1. Introduction

The microbial attachment and proliferation on biomedical surface significantly threaten the health of the patients.<sup>[1]</sup> Especially, the gathered microbes will form the impenetrable biofilm, which acts as a physical barrier to protect the bacteria from

the attack of immune system and drugs.[2] To relieve or even eliminate the threats, a series of antibacterial surfaces have been developed.<sup>[3]</sup> The common design strategy includes: antifouling designs to avoid initial microbe adhesion<sup>[4]</sup> and antibacterial designs to kill the touched bacteria.<sup>[5]</sup> However, the stubborn live bacteria and dead bacteria are still present and influence the subsequent antibacterial performance. To release the attached bacteria, a series of stimulus-responsive chains are combined.<sup>[6]</sup> Specifically, bacteria release method is designed by utilizing the force from the stimuli-triggered chain extension and hydration. For example, Yin et al. have developed a hierarchical brush with an outer layer of poly(methacrylic acid) (PMMA) and an inner layer of antimicrobial peptides (AMP);[7] the hydrophilic PMAA could not only resist the initial bacteria adhesion, but also collapse under bacteria-triggered acidification to expose the inner bactericidal AMP or extend to release the attached bacteria under an

increased pH. Zhao et al. have designed an antibacterial surface composed of an antifouling polyzwitterionic bottom layer and a thermal-responsive poly(N-isopropylacrylamide) (PNIPAM)-based polymer upper layer buried with vancomycin (Van); the bactericidal Van was buried/exposed along with the thermal-triggered collapse/extension of the PNIPAM chains and the

Y. Wang, Y. Ni, J. Zhou, S. Wang, Y. Gu, S. Y. Zheng, J. Yang College of Materials Science & Engineering Zhejiang University of Technology Hangzhou 310014, P. R. China E-mail: zhengsiyu@zjut.edu.cn; yangjt@zjut.edu.cn G. Wang Department of Orthopedics Shanghai General Hospital Shanghai Jiao Tong University School of Medicine

The ORCID identification number(s) for the author(s) of this article can be found under https://doi.org/10.1002/admi.202201209.

© 2022 The Authors. Advanced Materials Interfaces published by Wiley-VCH GmbH. This is an open access article under the terms of the Creative Commons Attribution License, which permits use, distribution and reproduction in any medium, provided the original work is properly cited.

Hangzhou 310027, P. R. China

D. Zhang, J. Zheng

Department of Chemical

Biomolecular
and Corrosion Engineering
The University of Akron
Ohio 44325, United States
E-mail: zhengj@uakron.edu
Z. L. Wu, Q. Zheng
Ministry of Education Key Laboratory of Macromolecular Synthesis
and Functionalization
Department of Polymer Science and Engineering
Zheijang University

DOI: 10.1002/admi.202201209

Shanghai 200080, P. R. China

www.advmatinterfaces.de

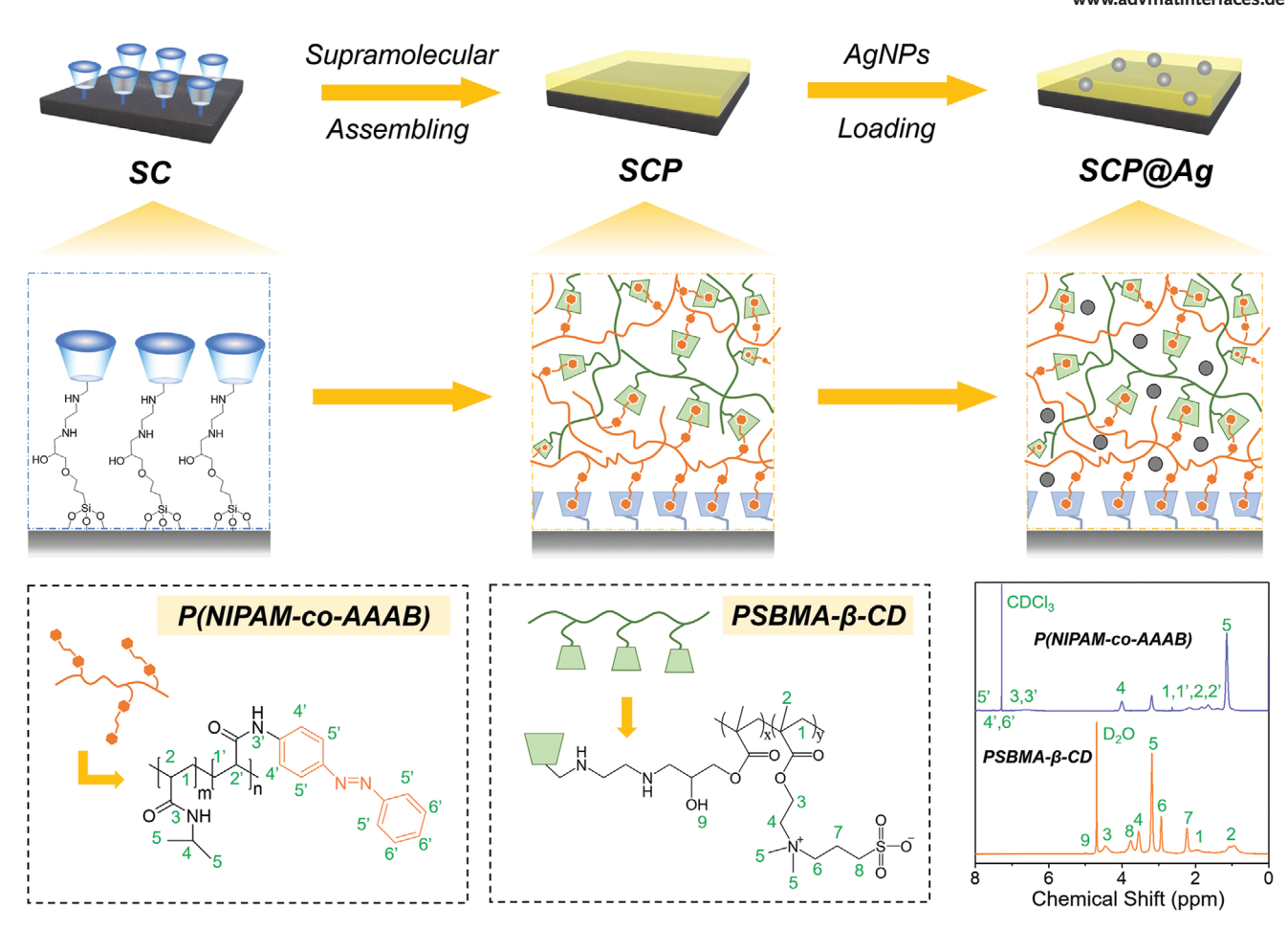


Figure 1. Preparation process of supramolecular antimicrobial coating with an illustration of the detailed chemical structure; The  $^{1}$ H-NMR spectrum of P(NIPAM-co-AAAB) (CDCl<sub>3</sub>), PSBMA-β-CD (D<sub>2</sub>O).

extension of PNIPAM chains also supposed to release ≈72.5% of the adhered bacteria. [8] Although these surfaces could release the attached microbe via the stimuli-triggered chain conformation change, they are usually triggered by contacting stimuli (pH, salts, temperature), which is still practically difficult or somewhat invasive. Besides, the limited bacterial release force might confine the release efficiency.

Different from the mentioned method, dissociation of a superficial layer based on switchable Schiff base motif,<sup>[9]</sup> borate ester bonds,[10] or host-guest interaction[11] could release the attached bacteria more thoroughly. For instance, Xu et al. have constructed an antibacterial surface by integrating antifouling polyethylene glycol (PEG) upper layer with bactericidal poly[2-(dimethyl decyl ammonium)ethyl methacrylatel (PODMAEMA) lower layer; [12] the two layers were bonded by Schiff base structure, which could be dissociated under the stimuli of bacteria metabolism to release the adhered bacteria. Chen et al. also developed a switchable Azobenzene (Azo)/\(\beta\)-cyclodextrin  $(\beta$ -CD)-mannose (CD-M) conjugates platform, which could kill bacteria and on-demand release captured bacteria by dissociating the Azo-modified molecules from the surface, with a bacterial release ratio of ≈95%.[13] Besides, our group also developed supramolecular comb-like polymer brushes via assembling the antifouling/antibacterial Azo-polymer on the hydrophilic CDspolymer backbone<sup>[14]</sup>; by dissociating the Azo-modified polymer branches under UV light, ≈85.1% of the attached bacteria was released. However, the sacrificing releasing method also has its shortcomings: 1) the dissociation of the bonds or specific structures usually needs more reaction time than chain movements, i.e., slower responsiveness; 2) reconstruction of the functional layer is often complicated, usually required of re-assembling the fresh molecules, i.e., not convenient for frequent use. Therefore, it is highly desired to develop a type of surface combined with both of fast release capability to ensure short-term, frequent use and thorough self-cleaning periodically to secure long-time antibacterial performance.

Herein, we developed a temperature/light dual-responsive antimicrobial gel coating based on host-guest recognition. Briefly, the CDs-modified surface was assembled in situ with CDs-contained antifouling poly(sulfobetaine methacrylate- $\beta$ -cyclodextrin) (PSBMA- $\beta$ -CD), Azo-contained thermal-responsive PNIPAM-based copolymer [P(NIPAM-co-AAAB)]; after that, bactericidal silver nanoparticles (AgNPs) was introduced into the network. The obtained supramolecular coating possessed a good antifouling performance with a low bacteria density of  $\approx 9.30 \times 10^5$  cells cm<sup>-2</sup> (*Escherichia coli*, 120 h), a high sterilization rate of  $\approx 96.9\%$ . By regulating the incubation temperature,  $\approx 86.9\%$  of the attached bacteria could be rapidly released via chain extension of PNIPAM segments; [16] the releasing rate could achieve  $\approx 91.0\%$  by further treating the surface with UV

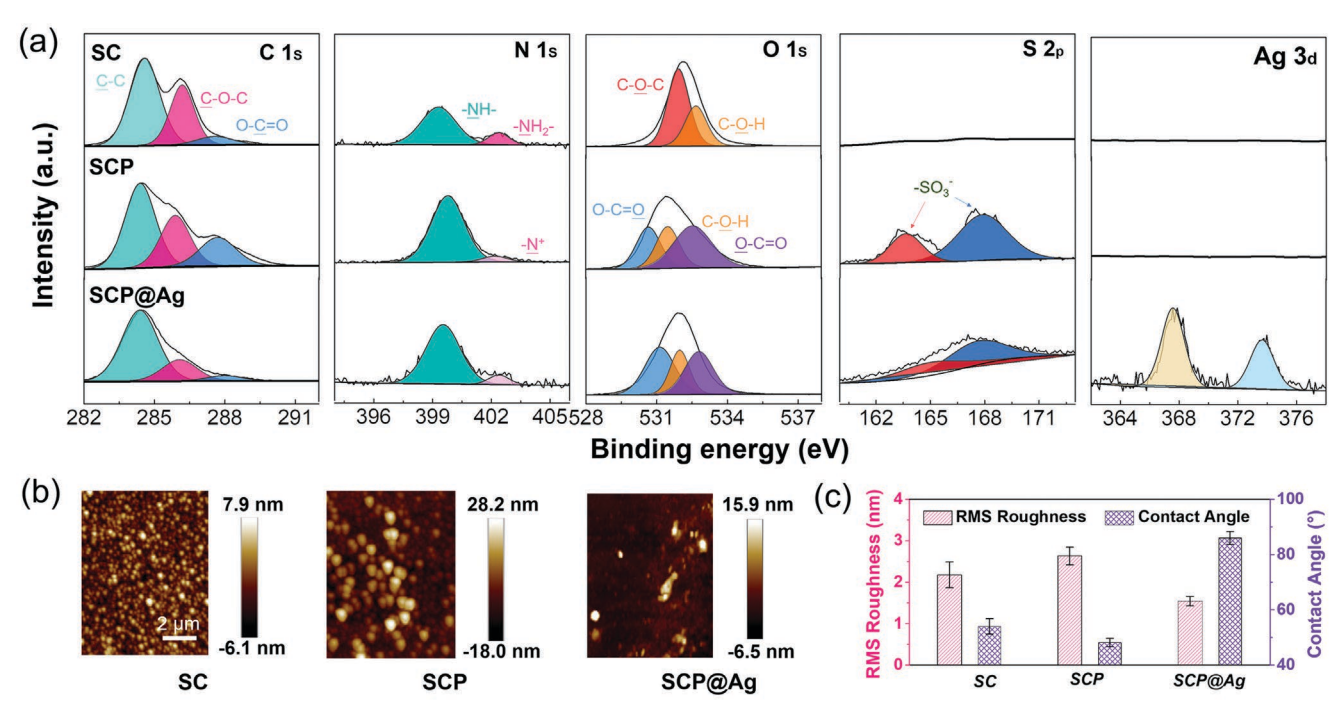


Figure 2. a) XPS spectra comparison for C1s, N1s, O1s, S2p, and Ag3d of SC, SCP, SCP@Ag surfaces. b) Representative AFM images of different surfaces (Scale bar:  $2 \mu m$ ). c) RMS Roughness and water contact angle values of different surfaces. The data was presented as the mean  $\pm$  SD (n = 3).

light to dissociate the coatings along with stubbornly attached bacteria. The surface after dissociation could be regenerated to resume the original multiple functions. The strategy illustrated here should provide a new insight into the design of smart antibacterial surface and broaden their applications.

# 2. Results And Discussion

The design strategy of the temperature/light dual-responsive antimicrobial surface as illustrated in Figure 1. First, the CDs-modified surfaces (SC) were prepared by sequential reacting with 3-Glycidoxypropyltrimethoxysilane (GPTMS) and Ethylenediamine-β-Cyclodextrin (EDA-β-CD) (Figure S1, Supporting Information). The host macromolecules PSBMA- $\beta$ -CD were synthesized by two-step method: firstly, copolymerizing of SBMA and glycidyl methacrylate (GMA), followed by ring-opening reacting of the GMA units with EDA- $\beta$ -CD. The guest macromolecules poly(N-isopropylacrylamide-coacrylamide azobenzene) P(NIPAM-co-AAAB) were obtained by directly copolymerizing the monomers of NIPAM and AAAB (Figure S2). After that, the SC surface was assembled with the aforementioned host/guest macromolecules to get a supramolecular gel coating (SCP). To endow the surface with bactericidal, AgNPs were loaded onto the coating through in situ reduction of silver ions (Ag+) and finally get the SCP@Ag surface. The chemical structure of the host/guest macromolecules and their immediate were verified by <sup>1</sup>H-NMR spectra (Figures 1 and S3, Supporting Information). The resulting supramolecular antimicrobial coating is supposed to display multiple functions including 1) the antifouling property originated from the hydrophilic polySBMA segments to resist initial bacterial attachment, 2) the bactericidal property provided by

AgNPs to kill the touched bacteria, 3) the thermal-responsiveness originated from the PNIPAM chain segments to release the attached bacteria, 4) the photo-responsiveness contributed by the PAAAB segments to further release the stubborn bacteria, 5) the surface regeneration function realized by switch the host-guest network.

The chemical/physical variation of the surface along with the preparation process was then investigated in detail (Figure S4, Supporting Information). As revealed by XPS spectra, the presence of the two N1s peaks in SC spectra (≈399.3 eV and ≈402.4 eV) was attributed to the reacted secondary amine and the unreacted primary amino of  $\beta$ -CDs, indicating successfully ring-opening reaction; the increment of signal (≈402.2 eV) in SCP was come from the additional quaternary ammonium groups on polySBMA segments (Figure 2a). The assembling of the PSBMA-β-CD was also confirmed by the S2p peaks at ≈163.7 eV (S=O) and ≈167.8 eV (S-O). After introducing AgNPs, two obvious peaks appeared in the Ag3d spectra, indicating the successful loading. Corresponding element content and XPS spectra of as-prepared surface were presented in Table S1 and Figure S5, Supporting Information. Atomic force microscopy (AFM) was employed to observe the surface morphology evolution of the surface. Compared to the as-prepared surface (Figure S6, Supporting Information), the root-mean-square (RMS) roughness of the SC surface increased to ≈2.18 nm with the emergence of small dark holes, demonstrating the successful graft of CDs (Figure 2b). The RMS roughness further increased to ≈2.63 nm after supramolecular assembling. Also, the surface become more hydrophilic after forming the antibacterial coating, with the minimum water contact angle (WCA) of ≈48.2° at SCP stage; the WCA was increased significantly to ≈86.0° after introducing hydrophobic AgNPs, consisting results of RMS roughness (Figure 2c).

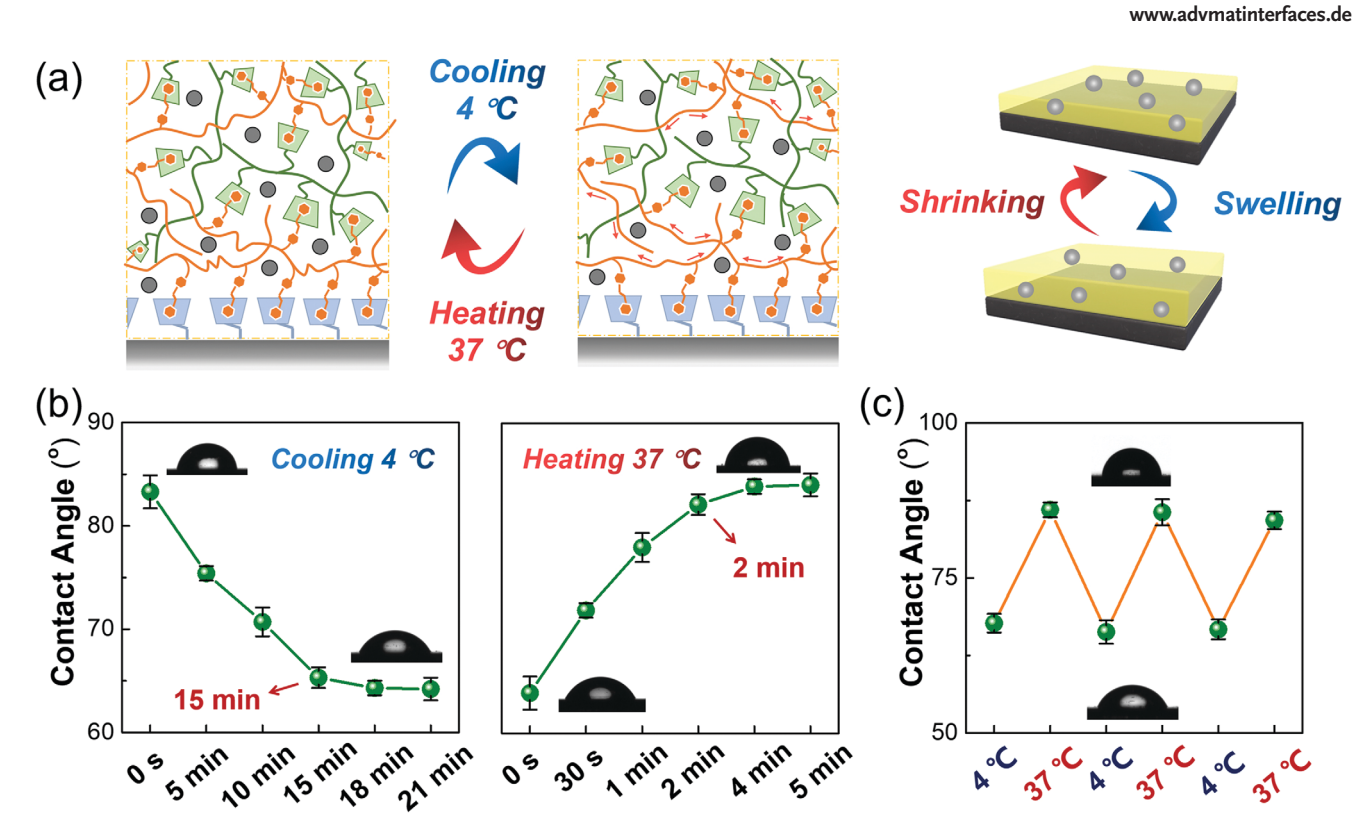


Figure 3. a) Schematic diagram of temperature responsiveness of gel network. b) Graph of water contact angle change under 4 °C and 37 °C along with the time. c) water contact angle changes after switching the temperature between 4 °C and 37 °C. The data was presented as the mean  $\pm$  SD (n = 3).

The thermal-responsiveness of the surface was then investigated. Owing to the hydration/dehydration of the PNIPAM segments beyond/below its transition temperature, the wettability of the surface was highly tunable by regulating the temperature (Figure 3a). As presented in Figure S7, Supporting Information, the thermal transition region of the coating was located within the temperature range of 15-35°C. Therefore, an extreme low temperature of 4 °C and a human body temperature of 37 °C was adopted as the tested temperature in our work. As illustrated in Figure 3b, the WCA of the surface was gradually decreased from ≈83.3° to ≈64.2° as the environmental temperature reduced to 4 °C, and increased back to its original level as the temperature returned to 37 °C. Such a switch of hydrated states could be repeated at least three times (Figure 3c). Corresponding photos of water contact angle were presented in Figure S8, Supporting Information.

The antibacterial performance of the obtained smart surface was systematically investigated via bacteria assay (Figure 4a-b). As shown in Figure 4c, the Gram-negative bacteria E. coli gathered on the surface during the elongation of incubated time. Specifically, the SCP surface showed excellent antifouling capability with the lowest bacteria density of  $2.27 \times 10^5$ cells cm<sup>-2</sup> after culturing for 120 h; introducing the AgNPs would compromise the antifouling behavior to some extent  $(9.30 \times 10^5 \text{ cells cm}^{-2})$ , yet improve the bactericidal performance significantly. As revealed in Figure 4d, the SC and SCP surfaces almost had negligible bactericidal properties with an antibacterial ratio of ≈6.8% and ≈8.0%, while that of the SCP@ Ag achieved ≈96.3%. Furthermore, the collapsed PNIPAM

segments in SCP and SCP@Ag coatings could be hydrated and extended at a low temperature of 4 °C, resulting in kicking off a great amount of the adhered bacteria. Compared to the negligible release ability of nonresponsive SC surface, ≈80.0% and ≈87.5% of the attached bacteria could be released from the SCP and SCP@Ag surfaces, respectively, by reducing the temperature to 4 °C. Corresponding antibacterial performance of the as-prepared surface was presented in Figure S9, Supporting Information. Similarly, the surface also showed great antibacterial behavior to the Gram-positive bacteria S. aureus. Specifically, the SCP@Ag surface exhibited low bacteria density of  $9.95 \times 10^5$  cells cm<sup>-2</sup> (culturing for 72 h) and could kill  $\approx 96.9\%$ of the attached bacteria, along with a high bacteria release ratio of ≈89.7% (Figure 4e-f).

It was worth noting that besides the temperature-responsiveness, The SCP@Ag surface also responded to the light due to the photo-switchable host-guest recognition. The photo-responsiveness of the host-guest interactions were widely studied to realize the sol-gel transition and self-healing, which was adopted for designing the injectable wound dressing.[11d,e] As revealed in Figure 5a-b, the characteristic peak of the azobenzene (at ≈350 nm) decreased from 0.64 to 0.25 as elongating the UV-irradiate time, indicating the transition of azobenzene from trans- to cis-form. Inversely, the absorbance of the peak could return to ≈0.63 by irradiating the 450 nm light. The photoisomerization of the azobenzene could be repeated for at least three cycles (Figure S10). As the result, the polymeric network was supposed to dissemble under the 365 nm light and reassemble in presence of fresh host-guest polymers

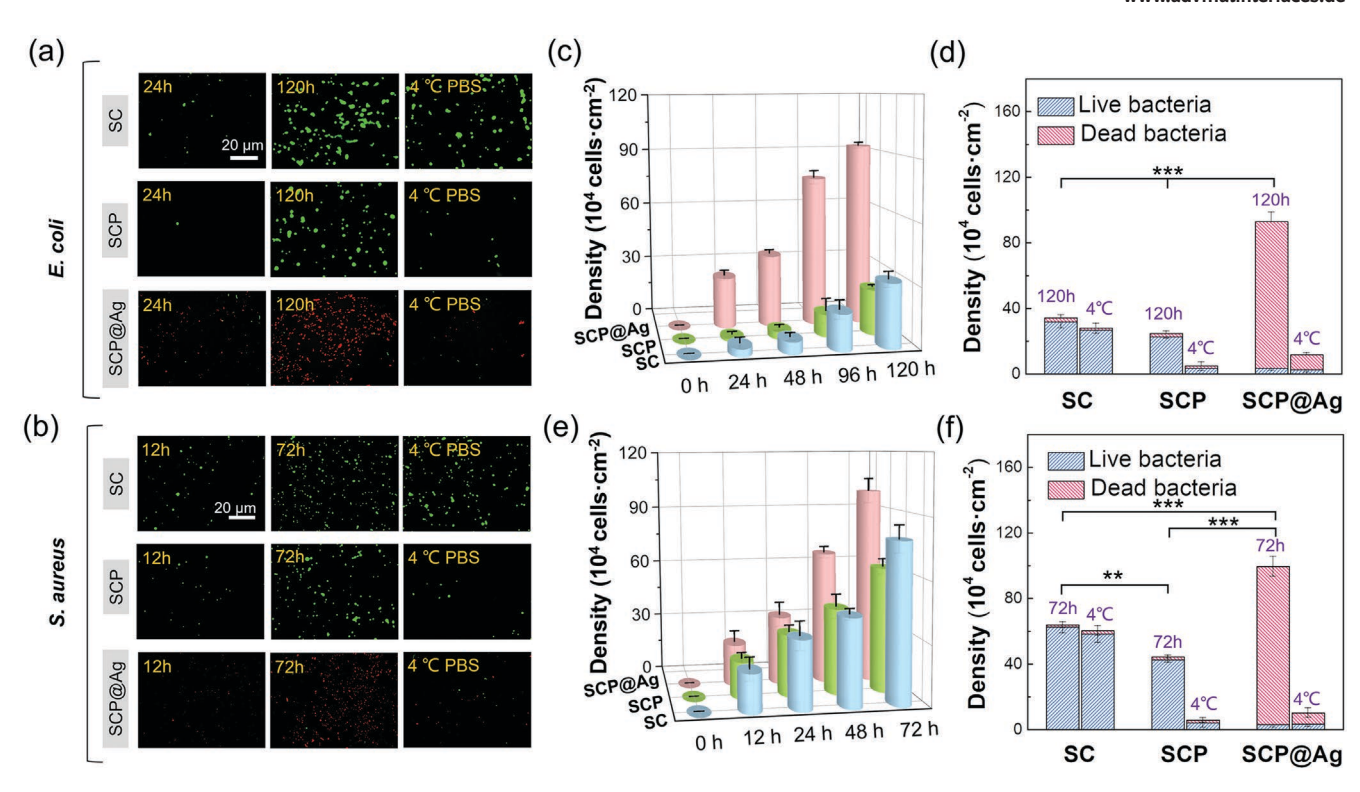


**Figure 4.** a–b) Representative fluorescence microscopy images of *E. coli* (a) and *S. aureus* (b) accumulation on SC, SCP, and SCP@Ag with different incubation times (Scale bar: 20  $\mu$ m). c) Statistical dynamics and d) live-/dead-bacterial statistics of adhered *E. coli*. e) Statistical dynamics and f) live-/dead-bacterial statistics of adhered *S. aureus*. The data was presented as the mean  $\pm$  SD (n = 3), and asterisks represent statistically significant differences (\*p < 0.05, \*\*p < 0.01, \*\*\*p < 0.001).

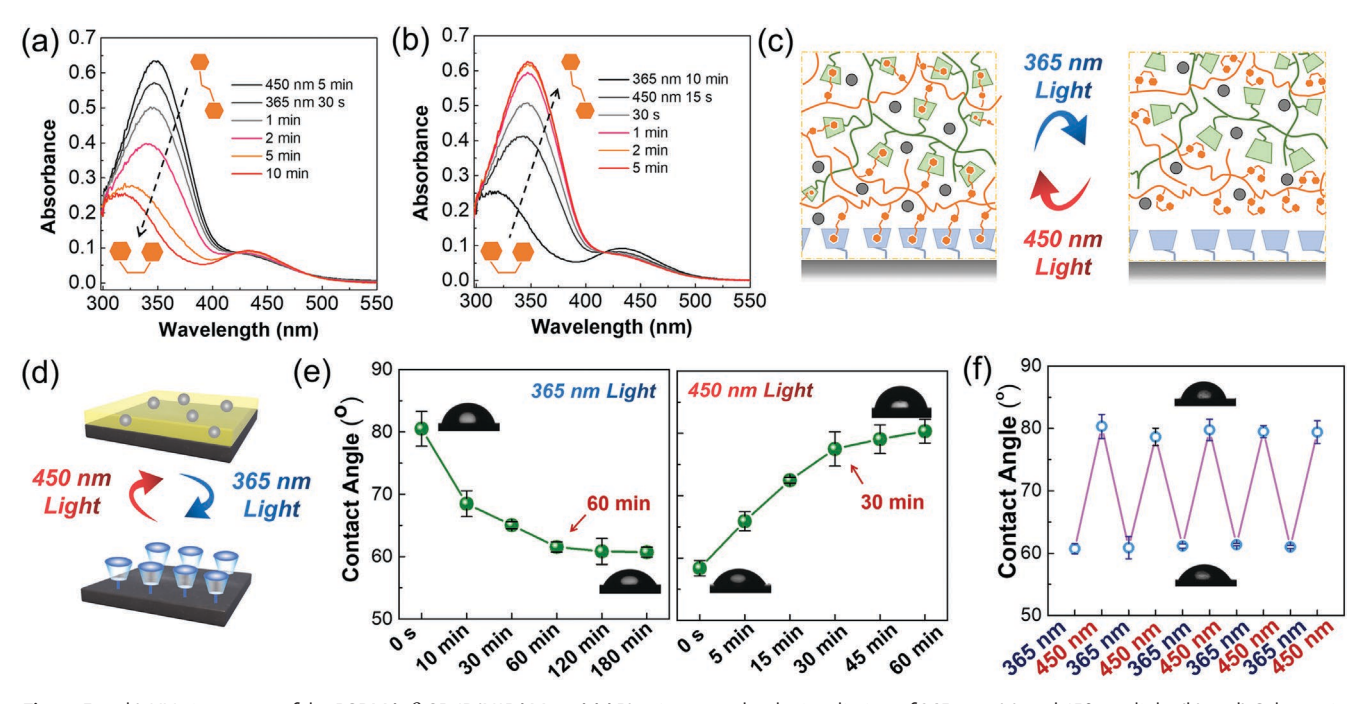


Figure 5. a-b) UV-vis spectra of the PSBMA- $\beta$ -CD/P(NIPAM-co-AAAB) mixture under the irradiation of 365 nm- (a) and 450 nm-light (b). c-d) Schematic illustration of the network structure change (c) and surface change (d) under the switch of the different light. e) Graph of water contact angle change under 365 nm- and 450 nm-light along with the time. f) water contact angle changes after switching the light between 365 nm- and 450 nm-light. The data was presented as the mean  $\pm$  SD (n = 3).

www.advmatinterfaces.de

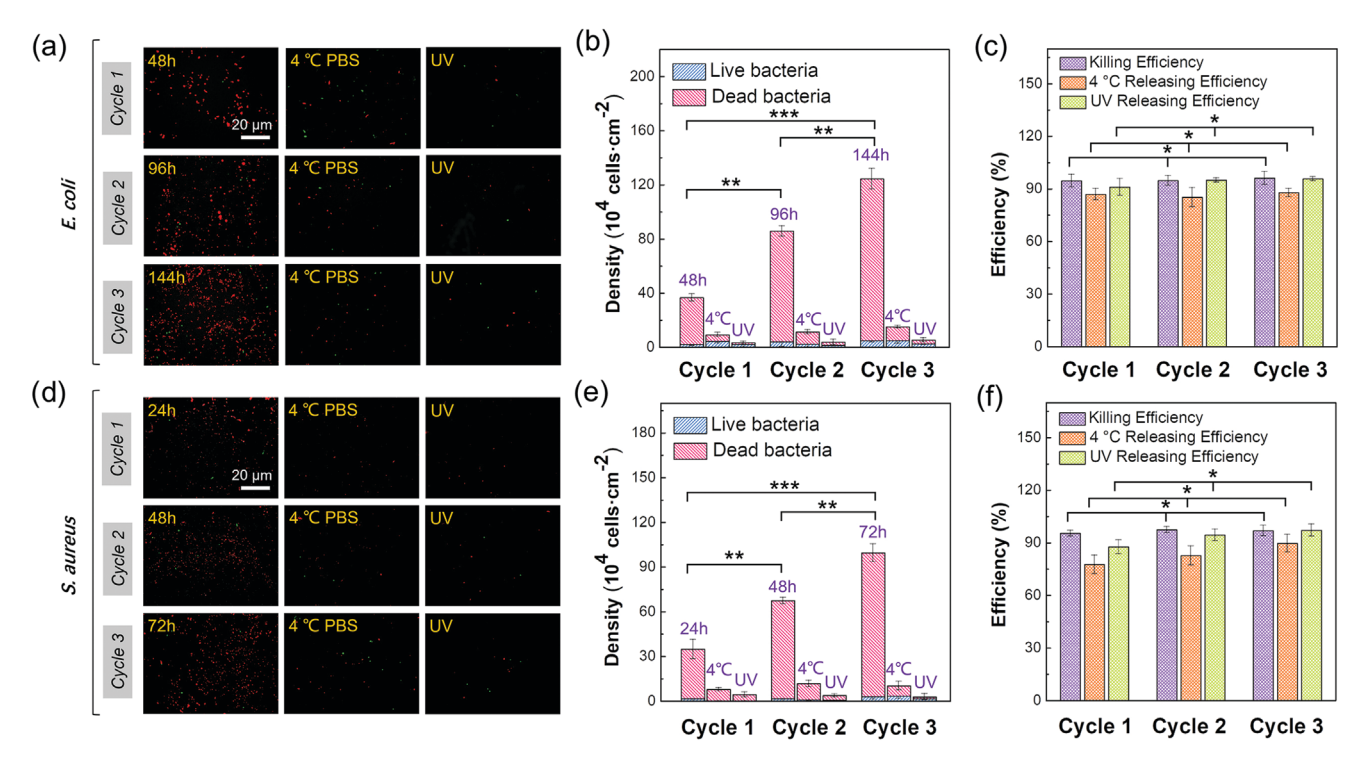


Figure 6. a) Representative fluorescence microscopy images of E. coli under cyclic response treatment and corresponding b) statistical live/dead cell analysis, c) release and killing efficiency of SCP@Ag surface; (Scale bar: 20 µm). d) Representative fluorescence microscopy images of S. aureus under cyclic response treatment and corresponding e) statistical live/dead cell analysis, f) release and killing efficiency of SCP@Ag surface; (Scale bar: 20 µm). The data was presented as the mean  $\pm$  SD (n = 3), and asterisks represent statistically significant differences (\*p < 0.05, \*\*p < 0.01), \*\*\*p < 0.001).

and 450 nm light based on the dissociation/association of the host-guest interactions (Figure 5c-d). The switch of the network structure was characterized by water contact tests. As shown in Figure 5e, the WCA of SCP@Ag surface (≈80.5°) was gradually decreased to ≈60.7° accordingly after irradiating with the 365 nm UV-light, which could resume by irradiation the 450 nm visible-light in soaking solutions. It was worth noting that the reconstruction time was kept at ≈30 min during the three successive surface regeneration (Figure S11, Supporting Information) and such dissociation-association process could be repeated without obvious diminish for at least five cycles (Figure 5f).

Thanks to such photo-switchable host-guest interactions, the residual bacteria after thermal-stimuli could be further released by dissociating the superficial layer; by soaking the fresh hostand guest-polymer chains with irradiation of 450 nm light, the antibacterial surface could be regenerated. As presented in Figure 6a, the 365 nm UV light could further improve the bacteria release ratio and the regenerated surface resumed the original capability pretty well for at least three cycles. As for the E. coli, the SCP@Ag could maintain the low bacteria density of  $12.4 \times 10^5$  cells cm<sup>-2</sup>, bacteria-killing ratio of  $\approx 95.0\%$ , thermaltriggered release rate of ≈87.8%, and photo-triggered release rate of  $\approx$ 95.7% after 3<sup>rd</sup> regeneration (Figure 6b-c). The surface exhibited similar antibacterial performance to S. aureus after 3<sup>rd</sup> regeneration (Figure 6d), including the low bacteria density of  $9.9 \times 10^5$  cells cm<sup>-2</sup>, bacteria-killing ratio of  $\approx 97.0\%$ , the thermal-triggered release rate of ≈89.7%, and photo-triggered release rate of ≈97.2% (Figure 6e-f). It was worth noting that the

bacterial releasing rate of the coatings in this work outperforms most existing works (Figure S12, Supporting Information). These results confirmed that the introduction of a host-guest was helpful to improve the bacteria release efficiency and cyclic surface regeneration.

# 3. Conclusions

In summary, we have prepared an antimicrobial coating composed of antifouling host polymers, thermal-responsive guest polymers, and bactericidal AgNPs based on photo-switchable host-guest recognition. The bactericidal rate of surface to E. coli/S. aureus reached ≈96.9%/≈97.5% and the surface resisted to the initial bacteria adhesion with a low bacterial density of  $\approx 9.30 \times 10^5 / \approx 9.95 \times 10^5$  cells cm<sup>-2</sup>. The surface could release ≈87.5%/≈89.7% of the E. coli/S. aureus in a cold environment. The residual bacteria could be further released with a dissociation of the host-guest interactions under UV light (bacteria release rate of ≈95.7%/≈97.2% for E. coli/S. aureus). Thanks to the switchable nature of the network, the surface could be regenerated to resume the functions with the assistance of soaking fresh host-/guest- polymers and irradiation of 450 nm light. The surface maintained low bacteria density of  $12.4 \times 10^5$  cells cm<sup>-2</sup>, bacteria-killing ratio of  $\approx 95.0\%$ , a thermaltriggered release rate of ≈87.8%, and a photo-triggered release rate of ≈95.7% even after 3<sup>rd</sup> regeneration. The strategy illustrated here would provide a new insight into the design of smart antibacterial surface and broaden their applications.



www.advancedsciencenews.com



www.advmatinterfaces.de

## 4. Experimental Section

Materials: β-Cyclodextrin (β-CD), p-tolunenesulfonyl chloride (TsCl), ethylenediamine (EDA), glycidyl methacrylate (GMA), sulfobetaine methacrylate (SBMA), 2,2'-azobis(2-methylpropionitrile) (AIBN), hydroquinone, acryloyl chloride were obtained from Aladdin. N-isopropylacrylamide (NIPAM) was purchased from Sigma-Aldrich. 3-Glycidoxypropyltrimethoxysilane (GPTMS), p-aminoazobenzene (Azo-NH $_2$ ) were obtained from Macklin. Acetonitrile, ethanol, methanol, toluene, benzene, tetrahydrofuran (THF), triethylamine (TEA), N, N-dimethylformamide (DMF), tetrahydrofuran (THF), sodium hydroxide (NaOH) were purchased from Linfeng Chemical Reagent Co., Ltd. Deionized water used in this project was obtained from a Millipore water purification system.

Synthesis of Copolymer P(SBMA-co-GMA): P(SBMA-co-GMA) copolymer was synthesized as reported in previous work.  $^{[17]}$  The monomers of SBMA (2.79 g, 10 mmol) and GMA (66.2  $\mu L$ , 0.5 mmol) were dissolved in a 50 mL round-bottom flask with 20 mL methanol/water (V/V = 1:1) solution under continuously stirring. After adding 1% eq of initiator AIBN (0.029 g), the homogeneous solution was degassed with  $N_2$  airflow for 15 min and then reacted for 6 h at 60 °C. The reaction was terminated by cooling in an ice-water bath for 3 h and white precipitates were collected. Subsequently, the white precipitate was redissolved in water and precipitated in methanol for three times. Finally, the purified product P(SBMA-co-GMA) was obtained by freeze-drying for 24 h.

Synthesis of Host Molecule PSBMA- $\beta$ -CD: PSBMA- $\beta$ -CD was synthesized via a ring-opening reaction with EDA- $\beta$ -CD. Briefly, copolymer of P(SBMA-co-GMA) (0.8 g) and EDA- $\beta$ -CD (0.5 g) were added into a 25 mL round-bottom flask with 10 mL deionized water. The ring-opening reaction was performed at 60 °C for 12 h. The product was obtained after dialysis the solution for 2–3 days (3500 Da, water) and then freeze-drying for 24 h.

Synthesis of Acrylamide Azobenzene (AAAB): The synthetic procedures of AAAB were similar as the previous report. Briefly, p-aminoazobenzene (11.25 mmol) and triethylamine (11.30 mmol) were dissolved in 30 mL of benzene. Then acryloyl chloride (13.90 mmol) and hydroquinone (0.64 mmol) were slowly added into the flask over 20 min and refluxed at 60 °C for 3 h. Afterward, the obtained solution was quenched in ice bath and removed the solvent using a rotary evaporator. The yellow powder AAAB was recrystallized in ethanol for three times and dried in a vacuum oven at 50 °C.

Synthesis of P(NIPAM-co-AAAB): The polymerization of the copolymer P(NIPAM-co-AAAB) followed a synthesis route as previously described.  $^{[1]b]}$  In brief, NIPAM (15.0 mmol), AAAB (0.15 mmol) and initiator AIBN (0.06 mmol) were sequentially added into a 50 mL round-bottom flask. THF (20 mL) was chosen as a solvent and the mixed solution was purged with a high-purity N $_2$  atmosphere for 15 min. After that, the sealed flask was immersed into an oil bath (60 °C) for 24 h and then used the ice bath to quench the reaction. Finally, the yellow product was precipitated three times with ether and dried for 24 h.

Preparation of Epoxy Substrate (SG): Silicon wafer hydrophilic treatment: the 10 mm × 10 mm pure silicon waters were ultrasonic washed in enthanol and DI water for twice. Whereafter, the substrates were immersed into the fresh "piranha solution" ( $H_2SO_4/H_2O_2$  3:1 V/V) at 120 °C for ≈60 min to obtain hydrophilic groups, washed with DI water and dried in nitrogen atmosphere for standby application. Then the pretreated hydrophilic substrates were placed in the reactor containing 10% (V/V) GPTMS in anhydrous toluene and reacted at 80 °C for 12 h under a nitrogen atmosphere. The epoxy group modified SG surfaces were obtained after repeatedly rinsed with toluene, ethanol, and DI water, and dried with N₂ flow.

Preparation of SW-GPTMS/EDA-β-CD Surface (SC): The synthetic procedures for the preparation of β-CD-OTs and EDA-β-CD were referring to our previous work. [11b] The SG substrates were immersed in EDA-β-CD solution (20 mL DMF with 0.2 g EDA-β-CD) for 24 h (60 °C). After reaction, the CD-modified substrates (SC) were ultrasonic washed with DMF, ethanol, and DI water for twice, and dried under N<sub>2</sub> flow for standby use. [19]

Preparation of SC/P(NIPAM-co-AAAB)/PSBMA-β-CD Surface via Host-Guest Interaction (SCP): SC substrates were immersed into a functionalized host-guest mixed solution (0.2 g P(NIPAM-co-AAAB)/0.2 g PSBMA-β-CD, 20 mL DI water as solvent at room temperature), irradiated at 450 nm light for  $\approx$ 30 min to complete the photoisomerization of azobenzene molecules, and further incubated overnight to achieve the adsorption of SC/P(NIPAM-co-AAAB)/PSBMA-β-CD (SCP) surfaces. Finally, the modified substrates were ultrasonic washed with DI water for twice and dried with a N<sub>2</sub> flow.

Embedding Silver Nanoparticles into the SCP Surface (SCP@Ag): Generally, the SCP surfaces were soaked in a 0.01M freshly prepared AgNO<sub>3</sub> solution, and stirred in the dark for 1 h. Afterward, the surfaces were put into NaBH<sub>4</sub> solution (0.01M) and stirred in the dark for 15 min. The SCP@Ag samples were washed with water and dried with an N<sub>2</sub> flow<sup>[20]</sup>

Composition and Surface Characterization: The chemical structure of P(SBMA-co-GMA), PSBMA-β-CD, AAAB, and P(NIPAM-co-AAAB) were characterized by 400 MHz III NMR spectrometer (1H-NMR, AVANCE) using  $D_2O$  and  $CDCl_3$  as solvent. The surface chemical compositions of SG, SC, SCP, and SCP@Ag surfaces were analyzed by X-ray photoelectron spectroscopy (XPS, Axis Ultra DLD) using an Al K $\alpha$  X-ray source, emitting 300  $\times$  700  $\mu$ m<sup>2</sup> at 15 kV and 3 mA with an incident Angle of 45°. The absorbance change of photo-responsive P(NIPAM-co-AAAB)/PSBMA-β-CD mixed solution was characterized via UV-vis spectra (Lambd A750 USA) from 250 nm to 600 nm, and 450 nm/365 nm were selected as typical wavelengths to test photoisomerization of azobenzene. The surface morphology and RMS roughness were observed by scanning atomic force microscopy (AFM, Bruker Dimension) at the frequency of 170-180 kHz. The surface hydrophilicity was characterized via water contact angle measurement (CA, Dataphysics OCA30) with a droplet of 2 µL of deionized water at ambient temperature and the average value was obtained by measuring the substrates at five different positions.

In Vitro Bacterial Assay: Escherichia coli (E. coli) and Staphylococcus aureus (S. aureus) were used to examine the antibacterial performance of the surfaces. The surfaces were co-cultured with bacteria on Luria-Bertani (LB, OXOID) at 37 °C overnight. A single colony of each bacterium was used to inoculate 40 mL of LB separately under shaking at 37 °C overnight and then the cultures were diluted to the suitable optical densities of ≈0.1 (E. coli) and ≈0.05 (S. aureus) at 600 nm (the corresponding bacteria densities represented as  $2.53 \times 10^7$  CFU MI<sup>-1</sup> and  $1.14 \times 10^7$  CFU mL<sup>-1</sup> for E. coli and S. aureus, respectively). [21] All samples were sterilized with 75% ethanol solution and rinsed in PBS solution for ten minutes before put into a 12-well sterile plate. Subsequently, adding 3 mL of bacterial solution in every well and cultured at 37 °C (120 rpm) for a pre-specified time with different cycles. After culturing, the samples were divided into two parts i) the control group and ii) the experimental groups, the samples for testing the temperature and light release property were placed into 4 °C PBS solution (shaken for 15 min) and for further evaluation of light-triggered bacteria release under 365 nm UV light for 1 h. All samples were taken out, rinsed with PBS and dye the LIVE/DEAD BackLight Viability Kit (Thermo Fisher Scientific Inc., NY) for 15 min in the dark for imaging, and then observed using an Axio Observer A1 fluorescence micro-scope (Carl Zeiss Inc., Germany) with a 40× lens. To examine long-term antifouling, bactericidal, and surface regeneration reliability, repeated "'antifouling-killingreleasing" processes were conducted for three cycles. Three samples were randomly selected for imaging and bacteria density analysis was performed using the software Image]. Compared with live/dead bacteria before/after the treatment of 4 °C PBS solution/365 nm UV light, the corresponding killing and releasing efficiency could be calculated via the following equations:

Killing efficiency = 
$$\frac{N_{D0}}{N_{L0} + N_{D0}} \times 100\%$$
 (1)

Releasing efficiency = 
$$\left(1 - \frac{N_{L1} + N_{D1}}{N_{L0} + N_{D0}}\right) \times 100\%$$
 (2)



www.advancedsciencenews.com



www.advmatinterfaces.de

where  $N_{L0}$  and  $N_{D0}$  represented as the initial amount of the live and dead bacteria under the specific culture time, respectively, while  $N_{L1}$  and  $N_{D1}$  were denoted as the amount of the live and dead bacteria after the bacteria release

Statistical Analysis: Statistical analysis of data presented in this work had a sample size n=3 and was presented as mean  $\pm$  SD. Student t-test or One-way ANOVA was used to analyze statistical differences between multiple groups. \*P < 0.05, \*\*P < 0.01, \*\*\*P < 0.001 were considered to be statistically significant.

# **Supporting Information**

Supporting Information is available from the Wiley Online Library or from the author.

# Acknowledgements

J.Y. acknowledges the support from the National Natural Science Foundation of China (Nos. 52073255 and 51673175) and the Natural Science Foundation of Zhejiang Province (No. LZ20E030004 and LY16E030012). S.Y. Zheng thanks the support from MOE Key Laboratory of Macromolecular Synthesis and Functionalization, Zhejiang University (2021 MSF02). J.Z. thanks a financial support from NSF-1806138.

### **Conflict of Interest**

The authors declare no conflict of interest.

#### **Author Contributions**

Y.W., G.W., and Y.N. contributed equally to this work. Y.W., G.W., and Y.N. contributed equally. S.Y.Z., J.Z., and J.Y. supervised this project. Y.W., G.W., Y.N., J.Z., S.W., Y.G., and D.Z. carried out laboratory research and discussed the results. Y.N., S.Y.Z., Z.L.W., Q.Z., J.Z., and J.Y. wrote and revised the manuscript, while all authors gave comments.

## **Data Availability Statement**

The data that support the findings of this study are available in the supplementary material of this article.

### **Keywords**

antibacterial surfaces, coatings, host-guest interaction, smart materials

Received: May 31, 2022 Revised: June 28, 2022 Published online: August 22, 2022

[1] a) M. Stracy, O. Snitser, I. Yelin, Y. Amer, M. Parizade, R. Katz, G. Rimler, T. Wolf, E. Herzel, G. Koren, J. Kuint, B. Foxman, G. Chodick, V. Shalev, R. Kishony, Science 2022, 375, 889; b) J. Huo, Q. Jia, H. Huang, J. Zhang, P. Li, X. Dong, W. Huang, Chem. Soc. Rev. 2021, 5, 8762; c) D. Mao, F. Hu, Kenry, S. Ji, W. Wu, D. Ding, D. Kong, B. Liu, Adv. Mater. 2018, 30, 1706831.

- [2] a) A. Vishwakarma, F. Dang, A. Ferrell, H. A. Barton, A. Joy, J. Am. Chem. Soc. 2021, 143, 9440; b) M. Tang, C. Chen, J. Zhu, H. R. Allcock, C. A. Siedlecki, L.-C. Xu, Bioact. Mater. 2021, 6, 447; c) J. Hu, Y. Ding, B. Tao, Z. Yuan, Y. Yang, K. Xu, X. Li, P. liu, K. Cai, Bioact. Mater. 2022, 18, 228; d) E. N. Hayta, M. J. Ertelt, M. Kretschmer, O. Lieleg, Adv. Mater. Interfaces 2021, 8, 2101024.
- [3] a) S. M. Imani, L. Ladouceur, T. Marshall, R. Maclachlan, L. Soleymani, T. F. Didar, ACS Nano 2020, 14, 12341; b) C. Zhao, L. Zhou, M. Chiao, W. Yang, Adv. Colloid Interface Sci. 2020, 285, 102280.
- [4] a) Y. Zou, K. Lu, Y. Lin, Y. Wu, Y. Wang, L. Li, C. Huang, Y. Zhang, J. L. Brash, H. Chen, Q. Yu, ACS Appl. Mater. Interfaces 2021, 13, 45191; b) S. Wang, D. Zhang, X. He, J. Yuan, W. Que, Y. Yang, I. Protsak, X. Huang, C. Zhang, T. Lu, P. Pal, S. Liu, S. Y. Zheng, J. Yang, Chem. Eng. J. 2022, 438, 135607; c) Q. Zeng, Z. Huang, G. Cai, T. Wu, Adv. Mater. Interfaces 2021, 8, 16.
- [5] a) X. Shi, S. H. P. Sung, J. H. C. Chau, Y. Li, Z. Liu, R. T. K. Kwok, J. Liu, P. Xiao, J. Zhang, B. Liu, J. W. Y. Lam, B. Z. Tang, Small Methods 2020, 4, 2000046; b) G. Fichman, C. Andrews, N. L. Patel, J. P. Schneider, Adv. Mater. 2021, 33, 2103677.
- [6] a) Y. Yi, R. Jiang, Z. Liu, H. Dou, L. Song, L. Tian, W. Ming, L. Ren, J. Zhao, J. Hazard. Mater. 2022, 432, 128685; b) M. Yin, M. Yang, D. Yan, L. Yang, X. Wan, J. Xiao, Y. Yao, J. Luo, ACS Appl. Mater. Interfaces 2022, 14, 8847; c) T. Keplinger, E. Cabane, J. K. Berg, J. S. Segmehl, P. Bock, I. Burgert, Adv. Mater. Interfaces 2016, 3, 1600233.
- [7] S. Yan, H. Shi, L. Song, X. Wang, L. Liu, S. Luan, Y. Yang, J. Yin, ACS Appl. Mater. Interfaces 2016, 8, 24471.
- [8] X. Wang, S. Yan, L. Song, H. Shi, H. Yang, S. Luan, Y. Huang, J. Yin, A. F. Khan, J. Zhao, ACS Appl. Mater. Interfaces 2017, 9, 40930.
- [9] a) M. Li, H. Wang, X. Chen, S. Jin, W. Chen, Y. Meng, Y. Liu, Y. Guo,
   W. Jiang, X. Xu, B. Wang, Chem. Eng. J. 2020, 382, 122973; b) K. Lei,
   K. Wang, Y. Sun, Z. Zheng, X. Wang, Adv. Funct. Mater. 2021, 31, 2008010.
- [10] a) P. Deng, X. Liang, F. Chen, Y. Chen, J. Zhou, Appl. Mater. Today 2022, 26, 12; b) F. Lin, Z. Wang, Y. Shen, L. Tang, P. Zhang, Y. Wang, Y. Chen, B. Huang, B. Lu, J. Mater. Chem. A 2019, 7, 26442.
- [11] a) S. Yan, S. Chen, X. Gou, J. Yang, J. An, X. Jin, Y. W. Yang, L. Chen, H. Gao, Adv. Funct. Mater. 2019, 29, 1904683; b) Y. Ni, D. Zhang, Y. Wang, X. He, J. He, H. Wu, J. Yuan, D. Sha, L. Che, J. Tan, J. Yang, ACS Appl. Mater. Interfaces 2021, 13, 14543; c) H. Wang, C. N. Zhu, H. Zeng, X. Ji, T. Xie, X. Yan, Z. L. Wu, F. Huang, Adv. Mater. 2019, 31, 1807328; d) Y. Wu, B. Guo, P. X. Ma, ACS Macro Lett. 2014, 3, 1145; e) R. Yu, Y. Yang, J. He, M. Li, B. Guo, Chem. Eng. J. 2021, 417, 128278.
- [12] Y. Zhang, X. Zhang, Y.-Q. Zhao, X.-Y. Zhang, X. Ding, X. Ding, B. Yu, S. Duan, F.-J. Xu, Biomater. Sci. 2020, 8, 997.
- [13] W. Zhan, T. Wei, L. Cao, C. Hu, Y. Qu, Q. Yu, H. Chen, ACS Appl. Mater. Interfaces 2017, 9, 3505.
- [14] S. Y. Zheng, Y. Ni, J. Zhou, Y. Gu, Y. Wang, J. Yuan, X. Wang, D. Zhang, S. Liu, J. Yang, J. Mater. Chem. B 2022, 1, 339.
- [15] a) F. A. Jerca, V. V. Jerca, R. Hoogenboom, Nat. Rev. Chem. 2022, 6, 51; b) H. B. Cheng, S. Zhang, J. Qi, X. J. Liang, J. Yoon, Adv. Mater. 2021, 33, 2007290.
- [16] a) C.-J. Kim, X. Hu, S.-J. Park, J. Am. Chem. Soc. 2016, 138, 14941;
  b) L. Tang, L. Wang, X. Yang, Y. Feng, Y. Li, W. Feng, Prog. Mater. Sci. 2021, 115, 100702.
- [17] Y.-N. Chou, T.-C. Wen, Y. Chang, Acta Biomater. 2016, 40, 78.
- [18] Z. Hu, Y. Liu, X. Xu, W. Yuan, L. Yang, Q. Shao, Z. Guo, T. Ding, Y. Huang, *Polymer* 2019, 164, 79.
- [19] J. Deng, X. Liu, W. Shi, C. Cheng, C. He, C. Zhao, ACS Macro Lett. 2014, 3, 1130.
- [20] R. Hu, G. Li, Y. Jiang, Y. Zhang, J.-J. Zou, L. Wang, X. Zhang, Langmuir 2013, 29, 3773.
- [21] L. Huang, L. Zhang, S. Xiao, Y. Yang, F. Chen, P. Fan, Z. Zhao, M. Zhong, J. Yang, Chem. Eng. J. 2018, 333, 1.